

THE HOT AND COLD SPOTS IN THE WMAP DATA ARE NOT HOT AND COLD ENOUGH

DAVID L. LARSON AND BENJAMIN D. WANDELT*

Department of Physics, University of Illinois at Urbana-Champaign, Urbana, IL 61801, USA
 Department of Astronomy, University of Illinois at Urbana-Champaign, Urbana, IL 61801, USA
Draft version May 23, 2019

ABSTRACT

This paper presents a frequentist analysis of the hot and cold spots of the Cosmic Microwave Background (CMB) data collected by the Wilkinson Microwave Anisotropy Probe (WMAP). We compare the WMAP temperature statistics of extrema (number of extrema, mean excursion, variance, skewness and kurtosis of the excursion) to Monte-Carlo simulations. We find that, on average, the local maxima (high temperatures in the anisotropy) are too cold and the local minima are too warm. In order to quantify this claim we describe a two-sided statistical hypothesis test which we advocate for other investigations of the Gaussianity hypothesis. Using this test we reject the isotropic Gaussian hypothesis at more than 99% confidence in a well-defined way. Our claims are based only on regions that are not excluded by the most conservative WMAP foreground mask. We perform our test separately on maxima and minima, and on the North and South Ecliptic and Galactic hemispheres and reject Gaussianity at above 95% confidence for almost all tests of the mean excursions. The same test also shows the variance of the maxima and minima to be low in the Ecliptic North (99% confidence), but consistent in the South; this effect is not as pronounced in the Galactic North and South hemispheres.

Subject headings: cosmic microwave background

1. INTRODUCTION

The WMAP data provides the most detailed data on the full sky CMB to date. This information about the initial density fluctuations in the universe allows us to test the cosmological standard model at unprecedented levels of detail. (Bennett et al. 2003b)

A question of fundamental importance to our understanding of the origins of the primordial seed perturbations is whether the CMB radiation is really an isotropic and highly Gaussian random field, as generic inflationary theories predict (Starobinsky 1982; Guth & Pi 1982; Bardeen et al. 1983).

A natural way to study the CMB is to look at the local extrema. This was initially suggested because the high signal-to-noise ratio at the hot spots means they would be detected first (Sazhin 1985; Vittorio & Juszkiewicz 1987; Bond & Efstathiou 1987). Heavens and Sheth calculate analytically the 2-point correlation function of the local extrema (1999). The high signal-to-noise ratio continues to make extrema attractive candidates for study.

We pursue this investigation by simulating Gaussian Monte-Carlo CMB skies, and comparing the WMAP data to those simulations. We choose several statistics and then check to see if the WMAP statistics lie in the middle of the Monte-Carlo distributions of statistics. We present results on the one-point functions of the local extrema: their number, mean excursion, and variance, skewness and kurtosis of the excursion.

The literature contains many other searches for non-Gaussianity, in the WMAP data and other CMB experiments. For example, Vielva et. al. detect non-Gaussianity in the 3- and 4-point wavelet moments (2003), and Eriksen et. al. find anisotropy in the n-

point functions of the CMB in different patches of the sky (2003). Others discuss possible methods of finding non-Gaussianity. Aliaga et. al. look at studying non-Gaussianity through spherical wavelets and “smooth tests of goodness-of-fit” (2003). Cabella et. al. review three methods of studying non-Gaussianity: through Minkowski functionals, spherical wavelets, and the spherical harmonics (2004). They propose a way to combine these methods. Chiang et. al. look at phase correlations among the spherical harmonics of the CMB (2002a; 2002b) Komatsu et. al. discuss a fast way to test the bispectrum for primordial non-Gaussianity in the CMB (2003b), and do not detect it (2003a). To this work, we add a strong detection of non-Gaussianity based on generic features: the local extrema.

The paper is laid out as follows. The next section discusses our method for making Monte-Carlo simulations of the CMB sky and calculating statistics on both the simulations and the WMAP data. It also explains our statistical tests. The third section describes our results. We conclude in section four.

2. METHOD

We test the WMAP data of the CMB sky by comparing the one-point statistics of its extrema to those same statistics on several sets of Monte-Carlo simulated Gaussian skies. Our initial hypothesis is that the statistics of the WMAP data are drawn from the same probability density function (PDF) as the statistics of the Monte-Carlo skies. If some WMAP one-point statistic falls lower or higher than most of the Monte-Carlo statistics, this indicates that our code may not correctly simulate the data and that our hypothesis may be false.

We examine several inputs to our Monte-Carlo simulation to see how those change the Monte-Carlo distribution of one-point statistics around the WMAP one-point statistics. We start very generally, looking at different

*B.D.W. is a 2003/4 NCSA faculty.
 Electronic address: dlarson1@uiuc.edu

frequency bands and galactic masks, and then narrow our search. Initially, we look at simulations including the three frequency bands (Q, V, and W) and the three published galactic masks for the WMAP data. Then we check to see if changing to a different published theoretical power spectrum affects our results. Finally, we look for anisotropy between the statistics of the Ecliptic and Galactic North and South hemispheres.

2.1. Monte-Carlo Simulation

A general outline of our Monte-Carlo simulation process follows. Each set of skies is labeled by its theoretical power spectrum, frequency band (Q, V, or W), and galactic mask. The frequency band determines both the (azimuthally averaged) beam shape function and noise properties on the sky. The simulated CMB skies are created as follows:

1. A Gaussian CMB sky is created with **synfast**, using a power spectrum and a beam function. The HEALPix (Górski et al. 1999a) pixelization of the sphere is used, with `nside=512`.
2. Random Gaussian noise is added to the sky (at each pixel) according to the published noise characteristics of the band being simulated. The WMAP radiometers are characterized as having white Gaussian noise (Jarosik et al. 2003).
3. The monopole and dipole moments of the sky (outside of the chosen galactic mask) are removed.

We make no attempt to simulate any foregrounds, including the galaxy; our analysis ignores data inside a galactic mask and uses the cleaned maps published on LAMBDA (NASA 2003) (Legacy Archive for Microwave Background Data Analysis).

For each Monte-Carlo set, one of four power spectra is used. These are the power spectra published by the WMAP team on (NASA 2003). We primarily use the best fit (bf) theoretical power spectrum to a cold dark matter universe with a running spectral index using the WMAP, CBI, ACBAR, 2dF, and Lyman-alpha data. In addition, we check the unbinned power spectrum (wmap) directly measured by WMAP, the power law (pl) theoretical power spectrum fit to WMAP, CBI and ACBAR, and a running index (ri) theoretical power spectrum fit to WMAP, CBI and ACBAR. See (Spergel et al. 2003; Bennett et al. 2003b; NASA 2003) for more information.

The galactic masks used are the `kp0`, `kp2`, and `kp12` masks published by the WMAP team (Bennett et al. 2003a). To check for differences between the North and South Ecliptic hemispheres, we define additional masks that extend the `kp0` galactic mask to block either the North or South hemisphere as well. For example, the Ecliptic South (ES) mask blocks the Northern Ecliptic sky as well as the galaxy. As a control, we also extend the `kp0` mask for galactic North and South hemispheres (GN and GS) to bring the total number of masks up to seven: `kp0`, `kp2`, `kp12`, `GS`, `GN`, `ES`, `EN`.

We use the same masking and dipole removal procedure for the WMAP data as for the Monte-Carlo skies.

The WMAP data we use are the cleaned, published maps. They are published by channel, so we calculate an *unweighted* average over (for example) all four W band

channels to get a map for the W band. The noise variance is calculated accordingly. We compute an unweighted average of the maps so that we can combine the WMAP beam functions through a simple average. After averaging, we remove the mean and dipoles from the WMAP sky.

2.2. Analysis and Hypothesis Test

Our analysis of both the Monte-Carlo and WMAP skies involves the following:

1. Locate the local maxima and minima of the HEALPix grid using **hotspot**.
2. Discard the extrema blocked by the galactic mask.
3. Calculate the statistics (number, mean, variance, skewness, and kurtosis) on the temperatures of the maxima and minima.
4. Statistically analyze the significance of the position of the WMAP statistic among the Monte-Carlo statistics.

Because we consider only the 1-point statistics, we consider only the temperature values, not their locations.

We calculate our five statistics for the maxima and minima separately. The two statistics which are typically negative for the minima, the mean and skewness, are multiplied by -1 in our results, to make comparison with the maxima statistics more clear.

For the rest of this section, we explain the fourth step in detail. To simplify the discussion, we consider the analysis of only one statistic on either maxima or minima, as we analyze the results for each statistic separately.

Our Monte-Carlo simulations are binomial trials, where the statistic calculated on a simulation can lie either above or below the WMAP statistic. It lies below the WMAP statistic with probability p , and for some set of n trials, i of the trials will have statistics below the WMAP statistic. Given p , the probability of i is $P(i|p) = \frac{n!}{i!(n-i)!} p^i (1-p)^{n-i}$. The value $\hat{p} \equiv i/n$ is both an unbiased and maximum likelihood estimator of p .

We are interested in whether p is near 0 or 1, since that indicates that our hypothesis—that the WMAP statistic came from the same PDF as the Monte-Carlo statistics—may be false. Because we do not have an alternative distribution for the WMAP statistic that we can test against the Monte-Carlo distribution, we do not test our hypothesis as phrased. We only look at a hypothesis H_0 that claims p is in some interval, $p \in (\alpha/2, 1 - \alpha/2)$, where we have arbitrarily chosen $\alpha = 0.05$.

We devise a statistical test of this hypothesis. Given our experimental result i , we construct the $1 - \alpha = 95\%$ symmetric confidence interval for p , as described in (Kendall & Stuart 1973). If this confidence interval lies entirely within the interval $[0, \alpha/2]$ or entirely within $[1 - \alpha/2, 1]$ then we reject our hypothesis, H_0 .

We reject H_0 for no values of i when $n = 99$, for $i = 0$ or $i = 199$ when $n = 199$, for $0 \leq i \leq 15$ or $985 \leq i \leq 1000$ when $n = 1000$, and for $0 \leq i \leq 103$ or $4897 \leq i \leq 5000$ when $n = 5000$.

This interval is a “95%” confidence interval in the following frequentist, non-Bayesian, sense. Suppose we repeat the experiment (with the same number of Monte-Carlo runs, and the same WMAP data) many times and

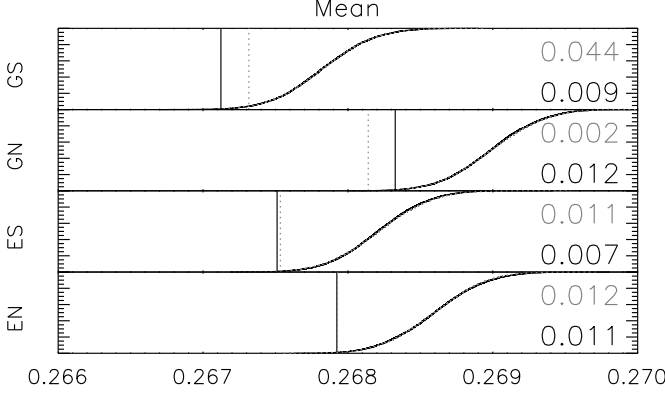


FIG. 1.— Cumulative distribution functions (CDFs) of mean temperature value (milli Kelvin) of the local extrema, found in sets of 5000 Monte-Carlo simulations for four galactic masks: GS, GN, ES, and EN. Best fit power spectrum and W band data are used. Means of the minima are negated for comparison. Maxima CDF is dotted while minima CDF is solid. Note their visual similarity. Statistics measured on WMAP data are shown as two vertical lines, dotted for maxima and solid for minima. Numbers on right are the same probabilities as in Table 1; for each pair, probability for the maxima is higher on the page.

get many values of i . We recalculate the confidence intervals each time, for each particular value of i . Ninety-five percent of the confidence intervals we calculate will contain the true value of p .

Our test is biased in favor of H_0 . Let H_1 be the alternative hypothesis $p \in [0, \alpha/2] \cup [1 - \alpha/2, 1]$. Then, for some values of p where H_1 is true (for example, $p = 0.02$, $n = 1000$), our test will choose H_0 more often than H_1 , given that i is a random variable with probability $P(i|p)$.

If desired, we can make the test unbiased by changing our value of α in the hypotheses H_0 and H_1 , but keeping the test (range of i for which H_0 is accepted) the same. For $n = 199$, we have an unbiased test if $\alpha = 0.00695$, for $n = 1000$, we have an unbiased test if $\alpha = 0.0313$, and for $n = 5000$, we have an unbiased test if $\alpha = 0.0415$. Note that all of these values are less than $\alpha = 0.05$. For any value of p , these tests are at least as likely to choose the correct hypothesis as the incorrect one. This is a 50% confidence, as opposed to our previous 95% confidence. This interpretation of the test does not change our results; it merely provides the different perspective that our test may be considered an unbiased 99.3% test, for $n = 199$, an unbiased 96.9% test, for $n = 1000$, or an unbiased 95.9% test, for $n = 5000$.

3. RESULTS

We display our results in Figure 1 and Table 1. The figure shows where the means of the WMAP maxima (and minima) lie in the Monte-Carlo cumulative distribution functions for that statistic. The table contains our estimates \hat{p} of p . When the result rejects the hypothesis H_0 , we print the value of \hat{p} in bold red.

We find that the mean temperature of the WMAP extrema, and in some cases the variance, differs significantly from the simulations, but number of extrema, skewness, and kurtosis are modeled fairly well by the

	A	B	C	D	0	1	2	3	4	5
bf	Q	kp0	max		.374	.000	.030	.566	.889	99
bf	Q	kp0	min		.010	.000	.232	.919	.707	
bf	Q	kp2	max		.333	.000	.152	.545	.899	99
bf	Q	kp2	min		.010	.000	.293	.919	.768	
bf	Q	kp12	max		.020	.000	.576	.929	1.000	99
bf	Q	kp12	min		.000	.000	.798	.919	1.000	
bf	V	kp0	max		.091	.616	.182	.495	.848	99
bf	V	kp0	min		.030	.182	.303	.990	.960	
bf	V	kp2	max		.061	.384	.061	.364	.727	99
bf	V	kp2	min		.040	.202	.263	1.000	.960	
bf	V	kp12	max		.000	.384	.212	.343	.889	99
bf	V	kp12	min		.020	.232	.444	.980	1.000	
bf	W	kp0	max		.475	.000	.141	.364	.475	99
bf	W	kp0	min		.414	.000	.343	.879	.646	
bf	W	kp2	max		.495	.000	.131	.182	.283	99
bf	W	kp2	min		.293	.000	.323	.808	.616	
bf	W	kp12	max		.434	.000	.242	.313	.253	99
bf	W	kp12	min		.364	.010	.505	.707	.737	
pl	W	kp12	max		.427	.000	.211	.307	.302	199
pl	W	kp12	min		.412	.005	.487	.734	.764	
ri	W	kp12	max		.342	.000	.271	.095	.136	199
ri	W	kp12	min		.337	.010	.769	.688	.663	
wmap	W	GS	max		.633	.023	.362	.045	.304	1000
wmap	W	GS	min		.685	.007	.981	.247	.213	
wmap	W	GN	max		.436	.000	.168	.504	.159	1000
wmap	W	GN	min		.243	.006	.060	.832	.610	
wmap	W	ES	max		.607	.010	.869	.103	.429	1000
wmap	W	ES	min		.176	.003	.923	.244	.152	
wmap	W	EN	max		.470	.011	.019	.416	.119	1000
wmap	W	EN	min		.702	.005	.067	.958	.861	
bf	W	GS	max		.603	.044	.240	.152	.434	5000
bf	W	GS	min		.641	.009	.852	.405	.284	
bf	W	GN	max		.371	.002	.091	.648	.284	5000
bf	W	GN	min		.209	.012	.035	.883	.697	
bf	W	ES	max		.560	.011	.472	.198	.487	5000
bf	W	ES	min		.151	.007	.586	.376	.253	
bf	W	EN	max		.436	.012	.002	.529	.188	5000
bf	W	EN	min		.668	.011	.011	.960	.869	

TABLE 1
ESTIMATED PROBABILITIES \hat{p} OF THE CMB STATISTICS BEING LESS THAN THE VALUE MEASURED BY WMAP, BASED ON SEVERAL MONTE-CARLO SAMPLINGS OF THOSE STATISTICS. COLUMN A GIVES THE POWER SPECTRUM: BEST FIT, POWER LAW, RUNNING INDEX, OR MEASURED UNBINNED WMAP. COLUMN B GIVES THE BAND USED, WHILE C TELLS THE MASK AND D TELLS WHETHER THE STATISTICS ARE FOR MINIMA OR MAXIMA. COLUMNS 0 THROUGH 4 GIVE AN UNBIASED ESTIMATE OF THE WMAP STATISTIC'S POSITION AMONG THE SORTED MONTE-CARLO SAMPLE STATISTICS. THE STATISTIC IN COLUMN 0 IS NUMBER OF HOT SPOTS. THE OTHER COLUMNS CORRESPOND TO: 1, MEAN; 2, VARIANCE; 3, SKEWNESS; AND 4, KURTOSIS OF EXTREMA TEMPERATURE VALUES. (FOR MINIMA, MEAN AND SKEWNESS STATISTICS ARE NEGATED BEFORE ESTIMATING PROBABILITY OF WMAP STATISTIC BEING LOWER.) COLUMN 5 GIVES THE NUMBER OF MONTE-CARLO SAMPLES CALCULATED. PROBABILITIES THAT INDICATE THAT, "THE TRUE VALUE OF p IS AT LEAST 95% LIKELY TO BE WITHIN 0.025 OF EITHER 0 OR 1," ARE IN RED BOLDFACE. THE TABLE SHOWS THAT THE DATA FALLS LOW IN THE MEAN TEMPERATURE DISTRIBUTION FOR ALMOST EVERY SET OF SIMULATIONS.

simulations. There is Ecliptic North-South asymmetry in the variance of the extrema.

For the mean, 2 out of our 4 results reject our hypothesis H_0 when $n = 199$, and all four of our results for the Ecliptic North and South hemispheres reject H_0 when $n = 1000$ and $n = 5000$. Since the statistics for the minima are negated, this means that the WMAP maxima are too cold and the WMAP minima are too hot. This is

a very significant result, regardless of whether our tests are considered 95% tests biased away from detection, or a 99.3%, a 96.9%, and a 95.9% test.

Even more significant are two 99% ($\alpha = 0.01$) level detections. In Table 1, they are rows bf, W, GN, max, mean; and bf, W, EN, max, variance. For this level of detection, we only accept values of i where $0 \leq i \leq 12$ or $4988 \leq i \leq 5000$. No 99% confidence detection was possible with only 1000 iterations.

The low magnitude of WMAP means is qualitatively observable in our initial ($n = 99$) simulations in the Q and W bands, but not the V band. We chose the W band to examine further because it had the best signal to noise ratio, and it had the least chance of foregrounds outside the kp0 mask that we use in our final analysis.

It has been suggested (Eriksen et al. 2003) that there is statistical anisotropy between the Ecliptic North and South hemispheres. We see this in the variance of the extrema temperatures. The Ecliptic North hemisphere has a statistically low variance (in one case at the 99% level) while the Ecliptic South is normal. To compare, we find the galactic North to be slightly low while the South is again normal.

4. CONCLUSION

In this paper we generate simulated CMB skies. We choose several statistics, and calculate them on both the simulations and the WMAP sky. We hypothesize that the WMAP statistics are drawn from the same distribution as the simulations' statistics, since we have attempted to accurately simulate the CMB sky. If the WMAP statistic is higher or lower than most of the simulations' statistics, this indicates that the WMAP statistic's underlying position $p \in [0, 1]$ in the distribution of Monte-Carlo statistics is close to 0 or 1. If we are 95% confident that p is within 0.025 of 0 or 1, then we claim the probability of the WMAP statistic happening by chance is sufficiently small to reject the hypothesis.

We find the WMAP data to have maxima which are significantly colder and minima which are significantly

warmer than predicted by Monte-Carlo simulation. For almost all simulations, we have 95% confidence that the mean of the WMAP hot spots or cold spots is in a 5% tail of the Monte-Carlo distribution. In one case, we are 99% confident the maxima statistic is in a 1% tail. Since we find the same lack of extreme temperature when we use the directly measured WMAP power spectrum, we are not simply restating that the WMAP power spectrum has a lack of power at large angular scales. The effect is independent of the galactic mask or power spectrum used.

We also find some anisotropy between the Ecliptic North and South hemispheres. The WMAP data in Northern hemisphere has a low variance statistic (95% confident that the variance statistic is in a 5% tail). In one case, we are 99% confident the variance of the maxima is in a 1% tail. There is less asymmetry between the North and South galactic hemispheres.

Our results may not be a detection of primordial non-Gaussianity. They could still be an effect of the WMAP instrument or data pipeline not modeled in our simulations or an as yet undiscovered foreground.

Our result is still highly significant. We have detected something, whether it is primordial non-Gaussianity or some other effect in the data. Having anomalous mean temperature values for the maxima and minima in both the North and South Ecliptic Hemispheres is unlikely to occur if the WMAP data were consistent with theoretical expectations.

We will present a complete treatment of the one and two point extrema statistics for the WMAP data set in a future publication.

Some of the results in this paper have been derived using the HEALPix (Górski, Hivon, and Wandelt 1999) package (Górski et al. 1999a,b). We would like to thank D. Spergel and O. Doré for reading a manuscript. This work was partially supported by the University of Illinois.

REFERENCES

- Aliaga, A., Martinez-Gonzalez, E., Cayon, L., Argueso, F., Sanz, J., Barreiro, R., & Gallegos, J. 2003, Tests of Gaussianity, astro-ph/0310706, proceedings of "The Cosmic Microwave Background and its Polarization", New Astronomy Reviews, (eds. S. Hanany and K.A. Olive), in press
- Bardeen, J. M., Steinhardt, P. J., & Turner, M. S. 1983, Phys. Rev. D., 28, 679
- Bennett, C., Hill, R. S., Hinshaw, G., Nolte, M. R., Odegard, N., Page, L., Spergel, D. N., Weiland, J. L., Wright, E. L., Halpern, M., Jarosik, N., Kogut, A., Limon, M., Meyer, S. S., Tucker, G. S., & Wollack, E. 2003a, ApJS, 148, 97
- Bennett, C. L., Halpern, M., Hinshaw, G., Jarosik, N., Kogut, A., Limon, M., Meyer, S. S., Page, L., Spergel, D. N., Tucker, G. S., Wollack, E., Wright, E. L., Barnes, C., Greason, M. R., Hill, R. S., Komatsu, E., Nolte, M. R., Odegard, N., Peirs, H. V., Verde, L., & Weiland, J. L. 2003b, ApJS, 148, 1
- Bond, J. R. & Efstathiou, G. 1987, MNRAS, 226, 655
- Cabella, P., Hansen, F., Marinucci, D., Pagano, D., & Vittorio, N. 2004, Search for non-Gaussianity in pixel, harmonic and wavelet space: compared and combined, astro-ph/0401307
- Chiang, L.-Y., Coles, P., & Naselsky, P. 2002a, MNRAS, 337, 488
- Chiang, L.-Y., Naselsky, P., & Coles, P. 2002b, astro-ph/0208235
- Eriksen, H. K., Hansen, F. K., & Banday, A. J. 2003, astro-ph/0307507
- Górski, K., Hivon, E., Reinecke, M., & Banday, A. 1999a, HEALPix, <http://www.eso.org/science/healpix/>
- Górski, K. M., Hivon, E., & Wandelt, B. D. 1999b, in Evolution of Large Scale Structure : from Recombination to Garching : Proceedings of the MPA-ESO Cosmology Conference, ed. A. J. Banday, R. K. Sheth, & L. N. D. Costa (Garching, Germany: PrintPartners Ipskamp)
- Guth, A. H. & Pi, S.-Y. 1982, Phys. Rev. Lett., 49, 1110
- Heavens, A. F. & Sheth, R. K. 1999, MNRAS, 310, 1062
- Jarosik, N., Barnes, C., Bennett, C. L., Halpern, M., Hinshaw, G., Kogut, A., Limon, M., Meyer, S. S., Page, L., Spergel, D. N., Tucker, G. S., Weiland, J. L., Wollack, E., & Wright, E. L. 2003, ApJS, 148, 29
- Kendall, M. G. & Stuart, A. 1973, The Advanced Theory of Statistics: Inference and Relationship, 3rd edn., Vol. 2 (New York: Hafner)
- Komatsu, E., Kogut, A., Nolte, M. R., Bennett, C. L., Halpern, M., Hinshaw, G., Jarosik, N., Limon, M., Meyer, S. S., Page, L., Spergel, D. N., Tucker, G. S., Verde, L., Wollack, E., & Wright, E. L. 2003a, ApJS, 148, 119
- Komatsu, E., Spergel, D. N., & Wandelt, B. D. 2003b, Measuring primordial non-Gaussianity in the cosmic microwave background, astro-ph/0305189
- NASA. 2003, LAMBDA, <http://lambda.gsfc.nasa.gov/>
- Sazhin, M. V. 1985, MNRAS, 216, 25P

- Spiegel, D. N., Verde, L., Peiris, H. V., Komatsu, E., Nolte, M. R., Bennett, C. L., Halpern, M., Hinshaw, G., Jarosik, N., Kogut, A., Limon, M., Meyer, S. S., Page, L., Tucker, G. S., Weiland, J. L., Wollack, E., & Wright, E. L. 2003, ApJS, 148, 175
- Starobinsky, A. A. 1982, Physics Letters, 117B, 175
- Vielva, P., Martínez-González, E., Barreiro, R. B., Sanz, J. L., & Cayón, L. 2003, astro-ph/0310273
- Vittorio, N. & Juskiewicz, R. 1987, ApJ, 314, L29